A General Coupling Matrix Synthesis Method for All-resonator Diplexers and Multiplexers

Yang Yu, *Student Member, IEEE,* Bo Liu, *Senior Member, IEEE,* Yi Wang, *Senior Member, IEEE,* Michael J. Lancaster, *Senior Member, IEEE* and Qingsha S. Cheng, *Senior Member, IEEE*

***Abstract*—Coupling matrix synthesis methods for all-resonator diplexers and multiplexers are far from mature. For complex coupling topologies, existing methods are often not able to find the appropriate coupling matrices that satisfy the S-parameter specifications. To address this challenge, a new synthesis method which hybridizes analytical and optimization techniques, called general all-resonator diplexer/multiplexer coupling matrix synthesis (GACMS) method, is proposed in this paper. The two main innovations of GACMS are: (1) An optimization framework incorporating filter design knowledge, which effectively reduces the search space for coupling matrix synthesis; and (2) A new memetic algorithm-based optimizer, which tackles the challenges from the complex landscape (function characteristics) of coupling matrix synthesis problems. GACMS is tested by six complex practical problems and coupling matrices are successfully obtained for all of them. Comparisons with existing methods demonstrate the advantages of GACMS in terms of solution quality and robustness.**

***Index Terms*—Coupling matrix, diplexers, multiplexers, differential evolution, memetic algorithm.**

I. Introduction

DIPLEXER and multiplexer design can often be divided into two phases, which are finding an initial 3D design with approximate geometric dimensions and then performing a full 3D electromagnetic (EM) simulation-based optimization. A good-quality initial design is essential for the second phase, no matter which local optimization-based methods [2] or global optimization-based methods [3] are employed. Using the Coupling Matrix (CM) provides a systematic method to obtain the initial design [1], [4], which is the focus of this paper.

The traditional types of junction-based diplexers or multiplexers usually use a non-resonant junction to connect with multiple channel filters. Analytical-based CM synthesis approaches are often employed. In such cases, the CM synthesis becomes multiple filter synthesis, which has been well documented [5]-[7]. Recently, an all-resonator multiple junction configuration was introduced and widely applied for various configurations of diplexers and multiplexers [8]-[11]. Fig. 1 shows an exemplary topology of an all-resonator multiplexer. The topology is exclusively comprised of coupled resonators. The configuration offers high flexibility, and various topologies can be realized by appropriately coupling the resonators. Clearly, traditional CM synthesis methods are no longer applicable [12]. This paper targets a general CM synthesis method for these all-resonator diplexers and multiplexers. The starting point of a diplexer / multiplexer design is an appropriate topology. Based on the chosen topology, the proposed method aims to obtain the coupling matrix that satisfies the S-parameter specifications. This is the same as in the analytical techniques, as there is no way to directly calculate the topology except for simple filters.

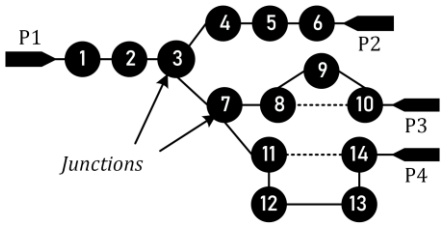

Fig. 1. An exemplary topology of an all-resonator multiplexer.

Existing CM synthesis methods can be classified into analytical-based methods and optimization-based methods. Exact analytical-based methods are mathematically sound and have guaranteed successful results. Hence, they are often the first choice. However, there is no available analytical method for many topologies such as the targeted all-resonator diplexers and multiplexers in this paper. In [12] and [13], a pioneering analytical method is proposed based on polynomial calculation and obtains successful results. However, this technique is only applicable to a particular type of all-resonator multiplexer. Optimization-based methods are a good choice for such cases due to their advantage of generality. For any CM, there is a corresponding S-parameter response, from which the errors to the S-parameter specifications can be calculated. By minimizing this error to a sufficiently small value, the appropriate coupling coefficients can be obtained.

There has been work on optimization techniques for CM synthesis. In [14], the CM for diplexers with a symmetric response is synthesized by the sequential quadratic

Manuscript received July 20, 2019. (corresponding author: B. Liu and Q. S. Cheng). This work is partially supported by the National Natural Science Foundation of China Grant 61471258 and by Science & Technology Innovation Committee of Shenzhen Municipality Grant KQJSCX20170328153625183. Partial support also comes from the UK Engineering and Physical Science Research Council under grant EP/S013113/1 and EP/M013529/1.

Y. Yu and Q. S. Cheng are with the Dept. of Electrical and Electronic Engineering, Southern University of Science and Technology, Shenzhen, 518055, P.R.China. (emails: issacyu@live.cn, chengqs@sustech.edu.cn).

Y. Yu, B. Liu, Y. Wang and M. J. Lancaster are with the School of Electrical, Electronic and System Engineering, University of Birmingham, Birmingham B15 2TT, U.K. (e-mail: yxy726@student.bham.ac.uk, b.liu.3@bham.ac.uk, y.wang.1@bham.ac.uk; m.j.lancaster@bham.ac.uk). B. Liu is also with James Watt School of Engineering, University of Glasgow, Glasgow, G12 8QQ, U.K (e-mail: bo.liu@glasgow.ac.uk).

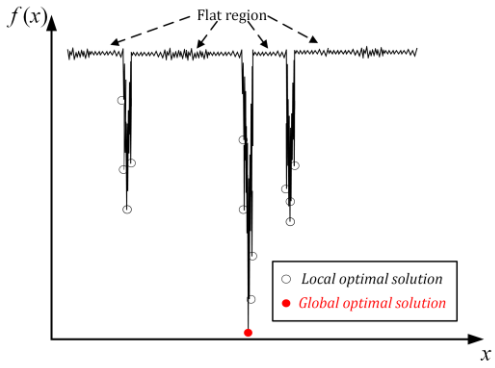

Fig. 2. An illustrative figure of the diplexer/multiplexer CM synthesis problem landscape. *x*: coupling coefficients, *f(x)*: objective function

programming (SQP) method with a starting point based on design experience. The method is extended to multiplexers in [8]. A global optimization technique, called self-adaptive differential evolution for CM synthesis (SADEC), is proposed in [15], which removes the dependence on a good-quality starting point. The search operators of SADEC are designed to fit for the landscape (function characteristics) of the diplexer CM. However, the above methods can be considerably improved and expanded, which is the aim of this work.

The landscape showing how the S-parameter performance-based objective function changes with respect to the coupling coefficients is complex for diplexers and multiplexers. A simplified representation of such a landscape is illustrated in Fig. 2 [15]. It can be seen that the global optimal value (the appropriate coupling coefficients in this case) locates in one narrow valley, as shown by the red point. The landscape has multiple narrow valleys. In each valley, the landscape is multimodal (i.e., with more than one local optimal solution, as marked out with circles) [15]. When the optimization is trapped at these points, an unsatisfactory result may be obtained.

Because of the complex landscape, optimization-based CM synthesis methods face two main challenges: (1) The number of coupling coefficients that can be handled is insufficient. Without being able to take advantage of an initial value, the SADEC algorithm would find it difficult in locating the solutions from an appropriate narrow valley for diplexers with more than 20 coupling coefficients [15]. However, many advanced diplexers and multiplexers have asymmetric responses and more than 20 coupling coefficients need to be handled. (2) Even if the appropriate valley is located, a suboptimal result may be obtained and the reflection responses may not reach the desired value (e.g., a 20 dB return loss) [14], [15].

To address the above challenges, a new method, called General All-resonator diplexers/multiplexers Coupling Matrix Synthesis (GACMS) method is proposed in this paper. The key idea is to hybridize analytical methods and advanced optimization techniques. In particular, design knowledge is employed to help reduce the search space as well as to provide useful supporting information (e.g., initial values for some coupling coefficients) for the optimization. In addition, new optimization techniques are developed to deal with the large number of local optima of the CM synthesis landscape and therefore considerably enhance the solution quality.

To test GACMS, six practical complex all-resonator diplexers and multiplexers are used. Successful results are obtained for all of them. Comparisons with existing methods show the advantages of GACMS in terms of solution quality and robustness. In addition, the proposed six test cases can serve as a benchmark set to evaluate and compare different CM synthesis algorithms.

The rest of this paper is organized as follows. Section II introduces the concepts of all-resonator diplexers and multiplexers and related fundamental optimization techniques. Section III describes the proposed GACMS method, including the new CM synthesis framework and the new optimization technique. Section IV describes the test cases. Numerical results and comparisons are provided in section V. Section VI concludes the paper.

II. The Problem Domain

A. Introduction to all-resonator diplexers and multiplexers

An example of an all-resonator diplexer is shown in Fig. 3. Typically, it can be divided into two parts, the stem and the branches [8]. The branches are coupled to the stem via junction resonators and each branch dominates one filtering band. Note that the branches share the junction resonator, as the junction resonator couples to and interacts with the branches. In general, all-resonator diplexers and multiplexers can be presented with a tree topology [8]. The number of couplings associated with each resonator is preferably no more than three. The port connecting to the stem (P1 in Fig. 3) is usually referred to as the common port [12], which passes all frequencies of the channel filters. It may be convenient to consider that the stem operates as a quasi-multiband bandpass filter [16]. Considering the resonators in the stem do not contribute to the isolation between the channels, the number of resonators in the stem should normally be kept minimum unless they are used to introduce transmission zeros as in [8]. More often, cross-couplings are added to the branches to generate transmission zeros and therefore enhance rejection and isolation [17], as is the case in Fig. 3.

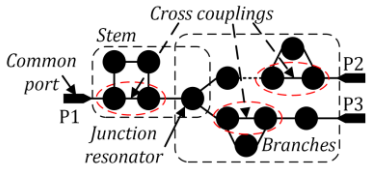

Fig. 3 The different parts of an all-resonator diplexer.

B. The coupling matrix for all-resonator diplexers and multiplexers

For an *n*-resonator network with *X* ($X \geq 3$) ports, the CM can be written in the form of block matrix $[M] \in \mathbb{R}^{(n+X)\times(n+X)}$ [16],

$$[M] = \begin{bmatrix} \boldsymbol{m} & \boldsymbol{m}_{n,PX} \\ \boldsymbol{m}_{n,PX}^{T} & \boldsymbol{0} \end{bmatrix}, \tag{1}$$

where $\boldsymbol{m} \in \mathbb{R}^{n\times n}$ is the general $n\times n$ CM, with the element $m(i, j)$ ($i \neq j$, and $i, j = 1, 2, \ldots, n$) the mutual coupling between resonators i and j, and the element $m(i, i)$ the self-coupling representing the resonant frequency of the i^{th} resonator. $\boldsymbol{m}_{n,PX} \in \mathbb{R}^{n\times X}$ is the matrix of external couplings between ports and resonators. The order of this CM is $n+X$. The corresponding normalized immittance matrix $[A]$ is given by [2]:

$$[A] = [R] + p[U] - j[M] \tag{2}$$

where $[R]$ and $[U]$ are block matrices,

$$[U] = \begin{bmatrix} \boldsymbol{u} & \boldsymbol{0} \\ \boldsymbol{0} & \boldsymbol{0} \end{bmatrix}, \quad [R] = \begin{bmatrix} \boldsymbol{0} & \boldsymbol{0} \\ \boldsymbol{0} & \boldsymbol{r} \end{bmatrix}, \tag{3}$$

where $\boldsymbol{u}$ is an $n\times n$ identity matrix and $\boldsymbol{r}$ is an $X\times X$ identity matrix. The S-parameters of this multi-port network can be calculated as

$$S_{pp} = \pm\left(1 - 2[A]^{-1}_{pp}\right), \tag{4}$$

$$S_{pq}\big|_{p\neq q} = 2[A]^{-1}_{pq}, \tag{5}$$

where S_{pp} is the reflection coefficient at the port attached to the p^{th} resonator, and S_{pq} is the transmission coefficient between the ports attached to the p^{th} and q^{th} resonators.

C. Available Optimization Techniques for CM Synthesis

As mentioned in Section I, SQP and SADEC have been employed and developed for diplexer and multiplexer CM synthesis. They are both used in GACMS and are briefly introduced below.

1) Sequence Quadratic Program

SQP is a popular local optimization technique for constrained nonlinear continuous problems and is used for CM synthesis [8-10]. In each iteration, the constrained optimization problem is modeled as a quadratic programming problem. The Lagrangian function for this problem is

$$L(x, \lambda_1, ..., \lambda_m) = f(x) + \sum_{i=1}^{m} \lambda_i^T c_i(x), \tag{6}$$

where $f(x)$ is the objective function, $c_i(x), i = 1, 2...m$ are the constraints and $\lambda_i, i = 1, 2, ...m$ are the Lagrange multipliers. In the t^{th} iteration of (6), the quadratic programming problem is

$$\begin{aligned} &\min_{x} \quad \nabla f(x_t)^T \cdot s_t + \frac{1}{2} s_t^T \nabla^2(L_t) \cdot s_t \\ &s.t. \quad \nabla c_i(x_t)^T s_t + c_i(x_t) \le 0, \; i = 1, 2, ..., m. \end{aligned} \tag{7}$$

where s_t is the solution to the quadratic programming problem. The next iteration has the form of

$$x_{t+1} = x_t + a_t \cdot s_t \tag{8}$$

where a_t is the step length obtained by a line search method. More details of the SQP method are in [19], [20].

2) SADEC

SADEC is an optimization algorithm specially designed for diplexer CM synthesis [15]. It is based on the differential evolution (DE) algorithm [18]. DE is a population-based stochastic global optimization algorithm. It starts by randomly initializing a population of candidate solutions. A mutation operator is then applied to generate a parent population P. In SADEC and GACMS, the DE/rand/1 operator [18] is used:

$$v^i = x^{r1} + F \cdot \left(x^{r2} - x^{r3}\right) \tag{9}$$

where x^{r1}, x^{r2}, and x^{r3} are three different candidate solutions randomly selected from the current population. v^i is the i^{th} mutation vector in the parent population. $F \in (0, 2]$ is a scaling factor. The method proceeds by applying a crossover operator to produce a child population. It works as follows.

i. Randomly select a variable index $j_{rand} \in \{1, \ldots, d\}$.

ii. For each $j = 1$ to d, generate a uniformly distributed random number *rand* from (0, 1) and set

$$u_j^i(t+1) = \begin{cases} v_j^i(t+1), & \text{if } (rand \le CR) \,|\, j = j_{rand} \\ x_j^i(t), & \text{otherwise} \end{cases} \tag{10}$$

where d is the number of variables, $CR \in [0, 1]$ is a constant called the crossover rate, and t is the number of iterations. Finally, a selection operator carries out a one-to-one competition between the parent population and the child population. The winners will become the initial population for the next iteration.

Considering the landscape of the diplexer CM synthesis, SADEC introduces self-adaptive strategies for the scaling factor F and the crossover rate CR. For F, this is

$$F_{temp} = \text{norm}(0.5, 0.25)$$

$$F^i(t) = \begin{cases} 1, & \text{if } F_{temp} > 1 \\ 0.1, & \text{if } F_{temp} < 0.1 \\ F_{temp}, & \text{otherwise} \end{cases} \tag{11}$$

where norm(0.5, 0.25) is a Gaussian distributed random number with a mean of 0.5 and a standard deviation of 0.25. The self-adaptive control of CR is

$$CR_{temp} = 0.1 + rand_1 \times 0.8$$

$$CR^i(t) = \begin{cases} CR_{temp}, & \text{if } rand_2 < 0.1 \\ CR^i(t-1), & \text{otherwise} \end{cases} \tag{12}$$

where t is the number of iterations. $CR(1)$=0.9 is chosen.

A new multi-population strategy is also introduced. Two opposite populations P and $\bar{P}$ are initialized and optimized together. These two populations have the following relations

$$\bar{x}^i(1) = a + b - x^i(1) \tag{13}$$

where the $[a, b]^d$ is the search range, d is the number of the decision variables (i.e., coupling coefficients), $x^i(1)$ is the i^{th} candidate solution in P and $\bar{x}^i(1)$ is the corresponding candidate solution in $\bar{P}$. The strategy to control the evolution of the two populations in the optimization process can be found in [15]. Experiments show clear improvement for SADEC compared to standard DE for the targeted problem. Equations (11)-(13) are also used in the GACMS method.

III. The GACMS Method

A. Challenges and Motivations

As stated above, the challenges of optimization-based diplexer / multiplexer CM synthesis mainly come from the landscape (Fig. 2 in Section I) [15], [21]. The search space grows exponentially with the increase in the number of coupling coefficients. Therefore, the valley where the global optimum lies appears even narrower with respect to the search space when more coupling coefficients are considered. In addition, our pilot studies show that when using cross-couplings, the number of local optimal solutions increases further. Hence, it is not a surprise that existing local and global optimization methods often have a low success rate for problems with more than 20 coupling coefficients [15].

To address the above challenges, two central ideas are proposed: (1) incorporating filter design knowledge to reduce the search space of the optimization, and (2) developing new optimization techniques to tackle the complex landscape (i.e., multimodal with narrow valleys).

By employing filter design knowledge, the whole diplexer / multiplexer structure can be divided into several smaller groups (i.e., the branches). The number of coupling coefficients for each of these is much smaller than the whole diplexer / multiplexer. A method can then be proposed to link these small groups to form the complete CM. This division also allows the employment of analytical methods to make initial estimations of some coupling coefficients, which narrows down the search ranges. We term these 'initial' values the 'FK values' because they are from Filter Knowledge. Based on the above ideas, a new CM synthesis framework is proposed, and the details are in Section III (B).

Our preliminary experiments show that even with the assistance of filter design knowledge, stronger optimization techniques are still needed to improve the solution quality. Global exploration is essential because being able to jump out of local optima either in the flat region or in the narrow valleys is critical. Local exploitation is also very important because of its ability to carry out an elaborate search in a certain region, so as to obtain a high-quality final CM.

Both local and global optimizers have been employed for CM synthesis in the literature [14], [15], but an optimizer with strong combined global and local optimization capabilities has not been proposed for the targeted problem to the best of our knowledge. Therefore, a new optimization algorithm integrating the advantages of local and global optimization is proposed here. The details are in Section III (C) after a detailed discussion of the full CM synthesis framework in the next subsection.

B. CM Synthesis Framework

The new CM synthesis framework integrating filter design knowledge with optimization is shown in Fig. 4. It works as follows:

Step 1: Normalization

The synthesis is carried out in a normalized frequency domain. The specifications are normalized by the well-known

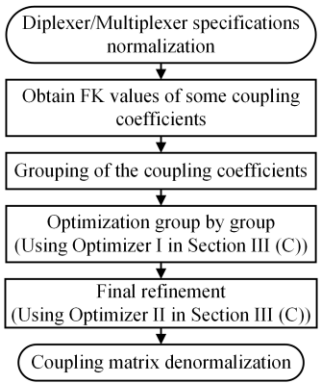

Fig. 4. The flowchart of the GACMS method.

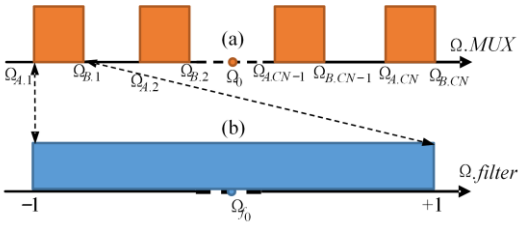

Fig. 5. Linear frequency transformation between (a) the normalized frequency domain of the multiplexer and (b) the lowpass prototype for each channel filter.

formulas in [6] and are not repeated here. Fig. 5(a) illustrates the frequency transformation of a multiplexer with *CN* channels. Each channel is represented by an orange block with $\Omega_{A,j}$ and $\Omega_{B,j}$, j (j = 1, …, *CN*) denoting the j^{th} channel. After normalization, the overall passband of the multiplexer will be projected to [−1, +1], namely $\Omega_{A.1} = -1$ and $\Omega_{B.CN} = +1$ in Fig. 5.

Step 2: Obtaining FK values of some coupling coefficients

The FK values for some coupling coefficients can be obtained by design knowledge. The goal is to narrow down the search ranges.

1) External couplings

The external couplings between the ports and their adjacent resonators are derived from the external quality factors of a series of hypothetical lowpass prototype filters (with band edges of ±1) as shown in Fig. 5(b). These filters have the same features (e.g., return loss, number of reflection zeros) as the channel responses of the diplexer / multiplexer. The external quality factors of the low-pass prototype filters can be calculated by the method in [4], [22]. Lowpass-to-bandpass frequency transformation is applied to the external quality factors of the lowpass prototype filters by:

$$q_{e.Pk} = q_{e.k}^{LP} \cdot \frac{2}{\left|\Omega_{A.j} - \Omega_{B.j}\right|}, (k = 2, ..., X;\ j = 1, ..., CN) \quad (14)$$

where $q_{e.Pk}$ and $q_{e.k}^{LP}$ denote the external quality factor of the k^{th} port in the multiplexer and their corresponding low pass prototype filter, respectively [14]. The external quality factor of the common port is then calculated by:

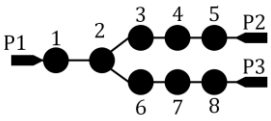

Fig. 6. An exemplary diplexer with 8 resonators.

$$\frac{1}{q_{e.P1}} = \sum_{k=2}^{X} \frac{1}{q_{e.Pk}} \tag{15}$$

Finally, the couplings between the ports and the resonators can be expressed as:

$$m(i, Pk) = 1/\sqrt{q_{e.Pk}}\,, (k = 1...X) \tag{16}$$

where the k^{th} port is coupled with the i^{th} resonator.

An as an example, an 8-resonator diplexer is shown in Fig. 6, assuming the following normalized specifications:

- Frequency ranges: Ch1 (−1 to −0.5) and Ch2 (0.6 to 1);
- Return loss level: 20 dB;

The couplings between the ports and resonators are calculated as $m(1, P1) = 0.1035$, $m(5, P2) = 0.2329$ and $m(8, P3) = 0.1863$ according to (14)-(16).

2) Mutual coupling coefficients

It is very difficult to find FK values for the coupling values associated with the stem part [14]. However, the FK values can be found for the branches employing bandpass filter CM synthesis methods. For any branch with all-pole responses, the FK values can be obtained by assuming a conventional two-port filter including the junction resonator. Therefore, the FK coupling values can be calculated from the g values of the low-pass prototype [4]. If cross-couplings exist, the analytical method [22] or the gradient-based optimization method [23] can be used to obtain the coupling coefficients. Then, a linear frequency transformation can be applied to transform from the lowpass back to the bandpass through

$$m_{u,v}^{BR} = m_{u,v}^{LP} \cdot \frac{\left|\Omega_{A.j} - \Omega_{B.j}\right|}{2} \; (j = 1...CN, u \neq v) \tag{17}$$

where $m_{u,v}^{BR}$ and $m_{u,v}^{LP}$ are the mutual couplings in branches and in the lowpass prototype filters, respectively. The self-couplings in the branches are obtained by:

$$m_{u,u}^{BR} = m_{u,u}^{LP} + \frac{\Omega_{A.j} + \Omega_{B.j}}{2} \; (j = 1\ to\ CN) \tag{18}$$

where $m_{u,u}^{BR}$ and $m_{u,u}^{LP}$ are the self-couplings of branches and lowpass prototype filters, respectively.

Taking the diplexer in Fig. 6 as an example, the obtained FK values are shown in Table I and the responses of the two branches after the above procedure are shown in Fig. 7.

Step 3: Grouping of the coupling coefficients

Since each branch mainly influences its corresponding channel response, it is reasonable to divide all the coefficients into groups [16]. In GACMS, all the couplings which have an influence on a channel constitute one group. Thus, the couplings in the stem are contained in every group. For the diplexer example in Fig. 6, the coupling coefficients are divided into two groups, as shown in Table II. Fig. 8 illustrates the group topologies after grouping.

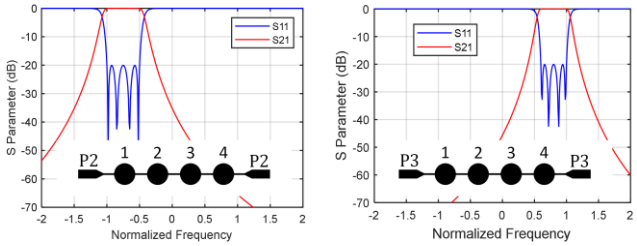

Fig. 7. The S-parameter responses of the two branches of filters

TABLE I
The FK values in each branch

Variables	$m(2, 3)$	$m(3, 4)$	$m(4, 5)$	$m(3, 3)$	$m(4, 4)$	$m(5, 5)$
Values	0.2279	0.1751	0.2279	−0.75	−0.75	−0.75
Variables	$m(2,6)$	$m(6,7)$	$m(7,8)$	$m(6,6)$	$m(7,7)$	$m(8, 8)$
Values	0.1823	0.1401	0.1823	0.8	0.8	0.8

TABLE II
Coupling coefficients in each group

Group	Coupling coefficients
Group 1	***m*(1, 2)**, $m(2, 3)$, $m(3,4)$,$m(4,5)$; ***m*(1, 1)**, ***m*(2, 2)**, $m(3, 3)$, $m(4, 4)$, $m(5, 5)$.
Group 2	***m*(1,2)**, $m(2,6)$, $m(6,7)$, $m(7,8)$; ***m*(1,1)**, ***m*(2,2)**, $m(6,6)$, $m(7,7)$, $m(8,8)$.

The bold ones are simultaneously in both groups.

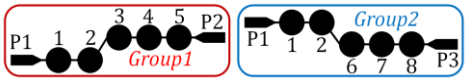

Fig. 8. Group topologies after coefficient grouping

Step 4: Optimization group by group

The FK values obtained in Step 2 will now be used in the following coupling coefficients group by group. Note that although a part of coupling coefficients are optimized in each group optimization, the objective function includes the specifications for all the channels. This allows solutions that improve the performance for some channels whilst not sacrificing the others. Details are in Section III (C).

The selection of which group to start is random. For the first group, the search ranges for the coupling coefficients in the stem are set as the full range, [0, 1]. The same applies to the coupling coefficients associated with the junction resonator. For other coupling coefficients in the targeted branch, the much narrower search range is set to be $[\boldsymbol{x}_h - r, \boldsymbol{x}_h + r]$, where $\boldsymbol{x}_h$ is the FK value vector and $r = 0.1$. Our pilot studies show that the value of 0.1 offers a good tradeoff between convergence speed and robustness.

It should be noticed that at the current stage, only the coupling coefficients in the first group are optimized, whereas the FK values in other groups are used as they are. The optimization outputs include the coupling coefficient values for the stem ($\boldsymbol{x}_s^{ref}$) and the targeted branch. It is observed that $\boldsymbol{x}_s^{ref}$ often has a small distance compared to the corresponding final optimal coupling coefficient value. Therefore, the search ranges for the coupling coefficients in the stem are scaled around $\boldsymbol{x}_s^{ref}$ in the following optimization. The optimization

algorithm used in this step, called Optimizer I, will be described in Section III (C).

For the subsequent groups, the optimizer does not change, but some search ranges are different. For the coupling coefficients in the stem, the search ranges are reduced to $[\boldsymbol{x}_s^{ref} - r, \boldsymbol{x}_s^{ref} + r]$. Again $r = 0.1$ is chosen. Note that $\boldsymbol{x}_s^{ref}$ is updated after the optimization of each group. For resonators uncoupled and coupled with the junction resonator in the currently targeted branch, the corresponding rules of selecting search ranges for the first group are used. For the coupling coefficients not in the targeted branch, they are not optimized and hold on the existing values (either FK values or optimized values). All the remaining groups' optimization will be executed following this process.

Step 5: Final refinement

Coupled with the junction resonators, the branches affect with each other due to the loading effect. Hence, the coupling coefficients after group by group optimization still need further improvement. In this step, they will be optimized as a whole but in a small range. A different optimizer, Optimizer II, is adopted, which will be described in Section III (C). After this final optimization, the obtained CM is transformed into the real frequency domain.

C. Optimization Techniques

1) Objective function

The objective function is critical for any optimization. For diplexer / multiplexer CM synthesis, the objective function is formed by *S*-parameter specifications. Assuming an *X*-port multiplexer, the objective function considered in this paper is

$$f(\boldsymbol{x}) = \frac{\sum_{k=1}^{X-1} \left|\max[S_{11}(PB_k)] - RL\right|}{\left|RL\right|} + \cdots + \frac{\left|\max[S_{32}(PB_1)] - IS\right| \cdots + \left|\max[S_{X,X-1}(PB_{X-1})] - IS\right|}{\left|IS\right|} \quad (19)$$

where PB_k denotes the k^{th} ($k = 1, \ldots, X-1$) passband. *RL* and *IS* are the desired return loss and isolation level, respectively. S_{11} is the reflection response of port 1 and S_{32}, S_{42}, …, $S_{X,X-1}$ represent the isolation responses.

The first term of (19) is related to S_{11}, representing the return loss of each channel. The value of S_{11} is evaluated from the CM by (4). The maximum values within the passbands are found to be $\max[S_{11}(PB_k)]$ in the objective function. Its distance to the desired return loss level (e.g., 20 dB) is minimized. The isolation response constraints (e.g., S_{32} in a diplexer) within the passbands are considered in the second term in (19). The design specifications for multiplexers usually demand the isolation within the passbands to be lower than the desired level (e.g., S_{32} of a diplexer is less than −30dB) [25]. It has been observed that the isolation response within the passband of one channel closely follows the transmission responses (e.g. S_{12}) in the rejection band of other channels [8], which helps to preserve the bandwidth within the passbands. Therefore, isolation responses within the passbands are used in the objective function as a convenient substitution for specifying the transmission responses. This also reduces the number of items in the objective function. Note that the optimal isolation response is largely determined by the selected topology. In a practical situation, if the isolation requirement cannot be met, an improved topology will be needed.

2) Optimizers I and II

As mentioned in Section III, Optimizer I is used in the group by group optimization in Step 4. This step requires the algorithm to find the narrow valley with the global optimum (see Fig. 2). To avoid being trapped in a wrong valley, a high global exploration ability is required. Moreover, because the valleys are very narrow, the new candidate solutions obtained by global exploration operators may be misplaced outside the valley (i.e., in the flat region in Fig. 2) even if the parent candidates have a good quality (e.g., x^{r1}, x^{r2}, and x^{r3} in (9)). Hence, local optimization is required to maintain the optimal search pattern obtained by global exploration while improving the objective function value.

Memetic algorithms are able to take into account the requirements for both global and local optimization. An evolutionary algorithm serves as the global optimizer, whereas the memetic algorithm integrates local optimization in the population update of the evolutionary algorithm [24]. In each iteration of the evolutionary algorithm, a part of or the whole population obtained by evolutionary operators is updated by local optimization, which serves as the starting population of the next iteration.

In GACMS, SADEC is selected as the global optimizer and SQP is selected as the local optimizer. SADEC shows a good capability to generate high-quality CMs for diplexers with symmetric responses without FK values [15]. SQP shows a good capability when good initial values of the CM are available [8]-[10]. In the proposed method, SQP is carried out for the whole population obtained by SADEC in each iteration. This memetic SADEC (MSADEC) is the Optimizer I used in Step 4 of the synthesis framework. Fig. 9 shows the flowchart of MSADEC. The self-adaptive mutation and crossover operator, as well as the return operator, are in (11)-(13) and more details are in [15].

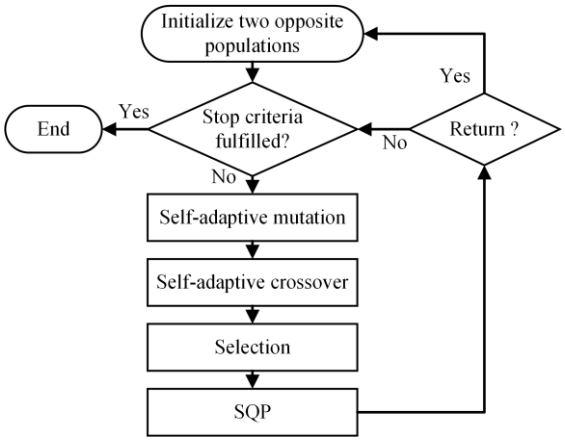

Fig. 9. The flowchart of MSADEC algorithm

SQP itself is used as the Optimizer II in Step 5. The search range is defined by ($\boldsymbol{m}_g$−0.1, $\boldsymbol{m}_g$+0.1), where $\boldsymbol{m}_g$ is the solution vector provided by Step 4. Note that $\boldsymbol{m}_g$ is often close to the final global optimal solution, and global exploration is not needed in this step. In addition, recall from Fig. 3 that the valley that contains the global optimal solution is very narrow. Using a global optimizer or SQP without restricting the search range may destroy the already obtained optimal pattern, which is verified by our pilot experiments. Hence, r=0.1 is used to restrict the local optimization.

IV. DIPLEXER AND MULTIPLEXER TEST CASES

This section provides six examples to test the GACMS method. These examples, shown in Fig. 10, are also proposed as test cases to serve as a reference for the community. For examples 2, 3 and 4, classical topologies with the same number of resonators can also produce a similar response and can be synthesized analytically. Here the corresponding all-resonator diplexers are used to verify the proposed method. Examples 1, 5 and 6, on the other hand, are meaningful to show because they allow many output ports (channels) maintaining the maximum number of couplings to each resonator to be 3. These examples demonstrate the unique advantages of the all-resonator configuration.

The complexity of the examples lies in the large number of resonators, the increasing number of channels (and therefore junction resonators), and the many cross-couplings. In particular, the FK values for the coupling coefficients associated with junction resonators are hard to obtain. A full search range (i.e., [0, 1]) for these couplings has to be used, which significantly increases the difficulty of optimization. The cross-couplings add more local optima, leading to a more rugged landscape. The test problems are of practical interest allowing entirely new designs of diplexers and multiplexers to be envisaged.

TABLE III
The key features of the test cases

Examples	No. of resonators	No. of channels	No. of cross-couplings	No. of variables (with FK values)
1	16	4	0	15 (12)
2	10	2	0	19 (16)
3	9	2	2	19 (19)
4	12	2	4	27 (24)
5	18	3	0	35 (26)
6	13	3	2	27 (24)

The key features of all the examples are listed in Table III. The specifications are expressed in the normalized frequency ranges for all cases.

Example 1 (Fig. 10 (a)) is a 16-resonator multiplexer with symmetric Chebyshev responses [8]. Symmetry helps reducing the number of variables to 15, the fewest among all the test

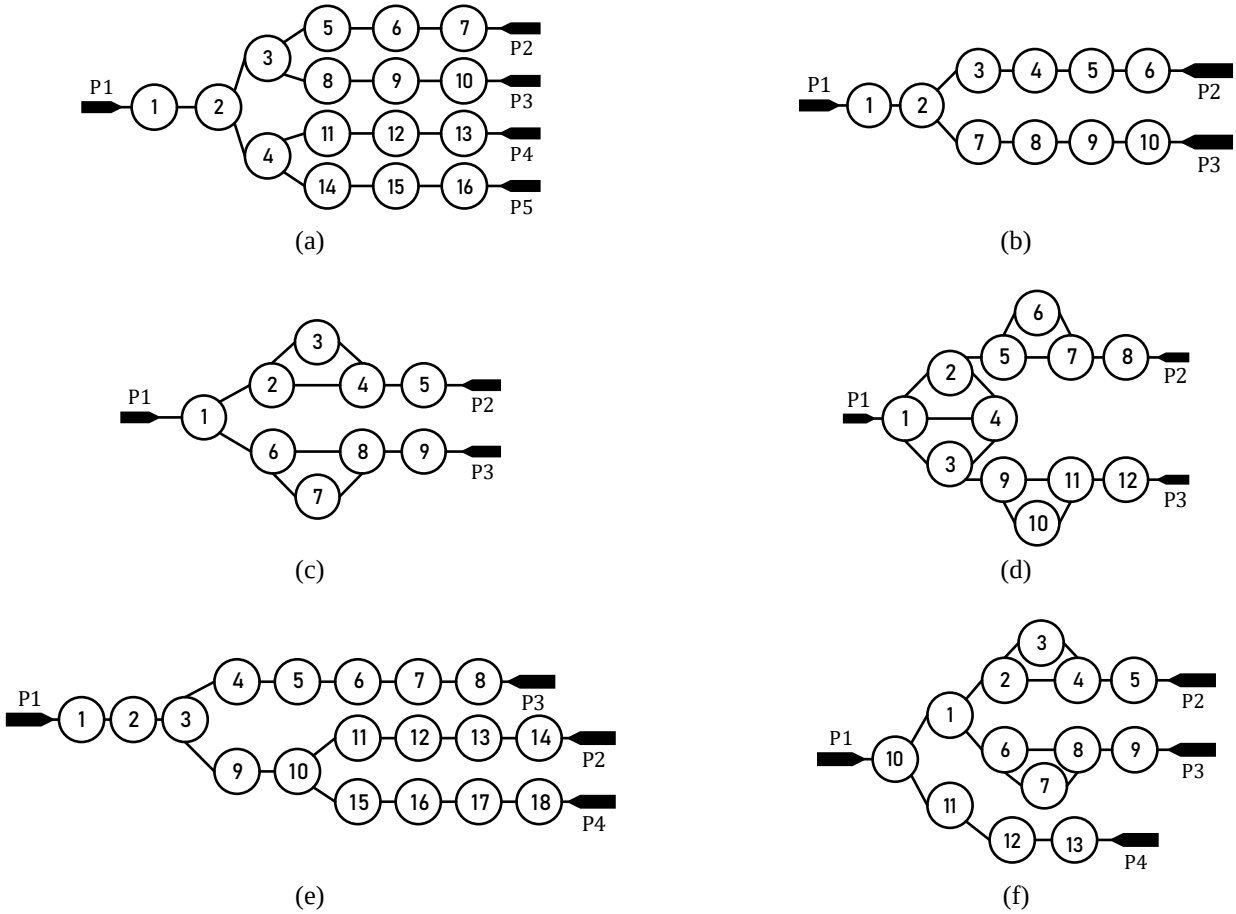

Fig. 10. The coupling topologies of the six test cases. (a) Example 1; (b) Example 2; (c) Example 3; (d) Example 4; (e) Example 5; (f) Example 6.

cases. The objective function is,

$$f_1 = \frac{\max(PB_1-(-20),0)}{20}+\frac{\max(PB_2-(-20),0)}{20} + \frac{\max(PB_3-(-20),0)}{20}+\frac{\max(PB_4-(-20),0)}{20} + \frac{\max(IS_1-(-30),0)}{30}+\frac{\max(IS_2-(-30),0)}{30} + \frac{\max(IS_3-(-30),0)}{30} \quad (20)$$

where PB_1=max(|S_{11}|), [−1, −0.75]; PB_2=max(|S_{11}|), [−0.417, −0.167]; PB_3=max(|S_{11}|), [0.167, 0.417]; PB_4=max(|S_{11}|), [0.75, 1]; IS_1=max(|S_{32}|), [0.167, 1]; IS_2=max(|S_{43}|), [−0.417, 0.417]; IS_3=max(|S_{54}|), [−1, −0.167]. PB_k denotes the k^{th} passband, the numbers in the square brackets refer to the normalized frequency bands. IS_j represents the j^{th} isolation level within the passbands. The following examples are represented by the same symbols.

Example 2 (Fig. 10 (b)) is a 10-resonator diplexer with asymmetric channel responses. The number of variables is 19. It has the same topology as in [15]. The objective function is

$$f_2 = \frac{\max(PB_1-(-20),0)}{20}+\frac{\max(PB_2-(-20),0)}{20} + \frac{\max(IS_1-(-80),0)}{80}+\frac{\max(IS_2-(-80),0)}{80} \quad (21)$$

where PB_1=max(|S_{11}|), [−1, −0.661]; PB_2=max(|S_{11}|), [0.709, 1]; IS_1=max(|S_{32}|), [−1, −0.661]; IS_2=max(|S_{32}|), [0.709, 1].

Example 3 (Fig. 10 (c)) is a 9-resonator diplexer. To realize a narrow guard band, each branch contains one triplet cross-coupling to generate one transmission zero. With the same number of variables, the optimization of this example is, however, more difficult than Example 2 due to the cross-couplings. The objective function is

$$f_3 = \frac{\max(PB_1-(-20),0)}{20}+\frac{\max(PB_2-(-20),0)}{20} + \frac{\max(IS_1-(-30),0)}{30}+\frac{\max(IS_2-(-30),0)}{30} \quad (22)$$

where PB_1=max(|S_{11}|), [−1, −0.203]; PB_2=max(|S_{11}|), [−0.026, 1]; IS_1=max(|S_{32}|), [−1, −0.203]; IS_2=max(|S_{32}|), [−0.026, 1].

Example 4 (Fig. 10 (d)) is a 12-resonator diplexer. The isolation response of all-resonator diplexers is not necessarily better than that of classical junction-based diplexers. This novel topology helps to increase the passband isolations of all-resonator diplexers [25]. Apart from the triplet in each channel, the coupling clusters 1-4 provide two extra transmission zeros. Both the number of decision variables and the cross-couplings increase the difficulty of optimization. The objective function is

$$f_4 = \frac{\max(PB_1-(-20),0)}{20}+\frac{\max(PB_2-(-20),0)}{20} + \frac{\max(IS_1-(-60),0)}{60}+\frac{\max(IS_2-(-60),0)}{60} \quad (23)$$

where PB_1=max(|S_{11}|), [−1, −0.1]; PB_2=max(|S_{11}|), [0.2, 1]; IS_1=max(|S_{32}|), [−1, −0.1]; IS_2=max(|S_{32}|), [0.2, 1]. The grouping of the coupling coefficients is shown in Table IV.

Example 5 (Fig. 10 (e)) is an 18-resonator triplexer comprised of standard Chebyshev filters. This topology has the largest number of resonators among all the examples. There are two junction resonators. The coupling coefficients associated with resonators 1 to 3 and 9 and 10 need to be searched in the full ranges without FK values. The objective function is

$$f_5 = \frac{\max(PB_1-(-20),0)}{20}+\frac{\max(PB_2-(-20),0)}{20} + \frac{\max(PB_3-(-20),0)}{20}+\frac{\max(IS_1-(-30),0)}{30} + \frac{\max(IS_2-(-30),0)}{30} \quad (24)$$

where PB_1=max(|S_{11}|), [−1, −0.6]; PB_2=max(|S_{11}|), [−0.25, 0.25]; PB_3=max(|S_{11}|), [0.4, 0.1]; IS_1=max(|S_{32}|), [−1, 0.25]; IS_2=max(|S_{43}|), [−0.25, 1]. The grouping of the coupling coefficients is shown in Table V.

Example 6 (Fig. 10 (f)) is a 13-resonator multiplexer. The guard band between the first two passbands is very narrow, while they are widely separated from the third band. Two cross-couplings exist in the first two branches which increase the difficulty of optimization. Moreover, the coupling coefficients associated with junction resonator 10 and 1 have to be searched in the full ranges without FK values. The objective function is

$$f_6 = \frac{\max(PB_1-(-20),0)}{20}+\frac{\max(PB_2-(-20),0)}{20} + \frac{\max(PB_3-(-20),0)}{20}+\frac{\max(IS_1-(-30),0)}{30} + \frac{\max(IS_2-(-30),0)}{30} \quad (25)$$

where PB_1=max(|S_{11}|), [−1, −0.578]; PB_2=max(|S_{11}|), [−0.485, −0.051]; PB_3=max(|S_{11}|), [0.684, 0.1]; IS_1=max(|S_{32}|), [−1, 0.051]; IS_2=max(|S_{43}|), [−0.485, 1]. The grouping of the coupling coefficients is shown in Table VI.

TABLE IV
The variables and group division of Example 4

No.	Coupling coefficients
Group 1	*m*(1,2), ***m*(1,4)**, *m*(2,4), *m*(2,5), *m*(5,6), *m*(6,7), *m*(7,8), *m*(5,7); ***m*(1,1)**, *m*(2,2), ***m*(4,4)**, *m*(5,5), *m*(6,6), *m*(7,7), *m*(8,8).
Group 2	*m*(1,3), ***m*(1,4)**, *m*(3,4), *m*(3,9), *m*(9,10), *m*(10,11), *m*(11,12), *m*(9,11); ***m*(1,1)**, *m*(3,3), ***m*(4,4)**, *m*(9,9), *m*(10,10), *m*(11,11), *m*(12,12).

The bold ones are simultaneously in both groups.

TABLE V
The variables and group division of example 5

No.	Coupling coefficients
Group 1	***m*(1,2)**, ***m*(2,3)**, *m*(3,4), *m*(4,5), *m*(5,6), *m*(6,7), *m*(7,8); ***m*(1,1)**, ***m*(2,2)**, ***m*(3,3)**, *m*(4,4), *m*(5,5), *m*(6,6), *m*(7,7), *m*(8,8).
Group 2	***m*(1,2)**, ***m*(2,3)**, ***m*(3,9)**, ***m*(9,10)**, *m*(10,11), *m*(11,12), *m*(12,13), *m*(13,14); ***m*(1,1)**, ***m*(2,2)**, ***m*(3,3)**, ***m*(9,9)**, ***m*(10,10)**, *m*(11,11), *m*(12,12), *m*(13,13), m(14,14).
Group 3	***m*(1,2), *m*(2,3)**, ***m*(3,9)**, ***m*(9,10)**, *m*(10,15), *m*(15,16), *m*(16,17), *m*(17,18); ***m*(1,1)**, ***m*(2,2)**, ***m*(3,3)**, ***m*(9,9)**, ***m*(10,10)**, *m*(15,15), *m*(16,16), *m*(17,17), *m*(18,18).

The bold ones are simultaneously in different groups.

TABLE VI
The variables and group division of example 6

No.	Coupling coefficients
Group 1	***m*(10,1)**, *m*(1,2), *m*(2,3), *m*(3,4), *m*(4,5), *m*(2,4); ***m*(10,10)**, ***m*(1,1)**, *m*(2,2), *m*(3,3), *m*(4,4), *m*(5,5).
Group 2	***m*(10,1)**, *m*(1,6), *m*(6,7), *m*(7,8), *m*(8,9), *m*(6,8); ***m*(10,10)**, ***m*(1,1)**, *m*(6,6), *m*(7,7), *m*(8,8), m(9,9).
Group 3	*m*(10,11), *m*(11,12), *m*(12,13); ***m*(10,10)**, *m*(11,11), *m*(12,12), *m*(13,13).

The bold ones are simultaneously in different groups.

V. Numerical Results and Comparisons

A. *Performance of GACMS*

GACMS is tested by the six cases in Section IV. In terms of parameter setting, there are two kinds: (1) Parameters in the synthesis framework, such as using $r = 0.1$ around FK values to define the updated search ranges: These parameters are set empirically, but once set, they are fixed within the framework and do not need to be altered by the user. (2) The algorithm parameters for the MSADEC optimizer: MSADEC does not introduce any new parameters compared with SADEC. Hence, the parameter setting for SADEC still applies to MSADEC, which is detailed in [15]. In the following experiments, the same SADEC parameters in [15] are used for MSADEC. For all the test examples, 10 runs are carried out for GACMS with independent random numbers. The maximum number of iterations for GACMS is 250. In most cases, satisfactory results are obtained within 150 iterations. The external coupling coefficients, the FK values and the typical final solutions for all the examples are shown in the Appendix. For all the examples, the CM synthesis time is around 20 to 30 minutes using a desktop computer with Intel i7-7770HQ CPU and 32 GB RAM.

The statistics of the GACMS results over 10 runs are shown in Table VII. The final responses are shown in Fig. 11. For test cases 2, 4 and 6, the optimal solutions fully satisfy the

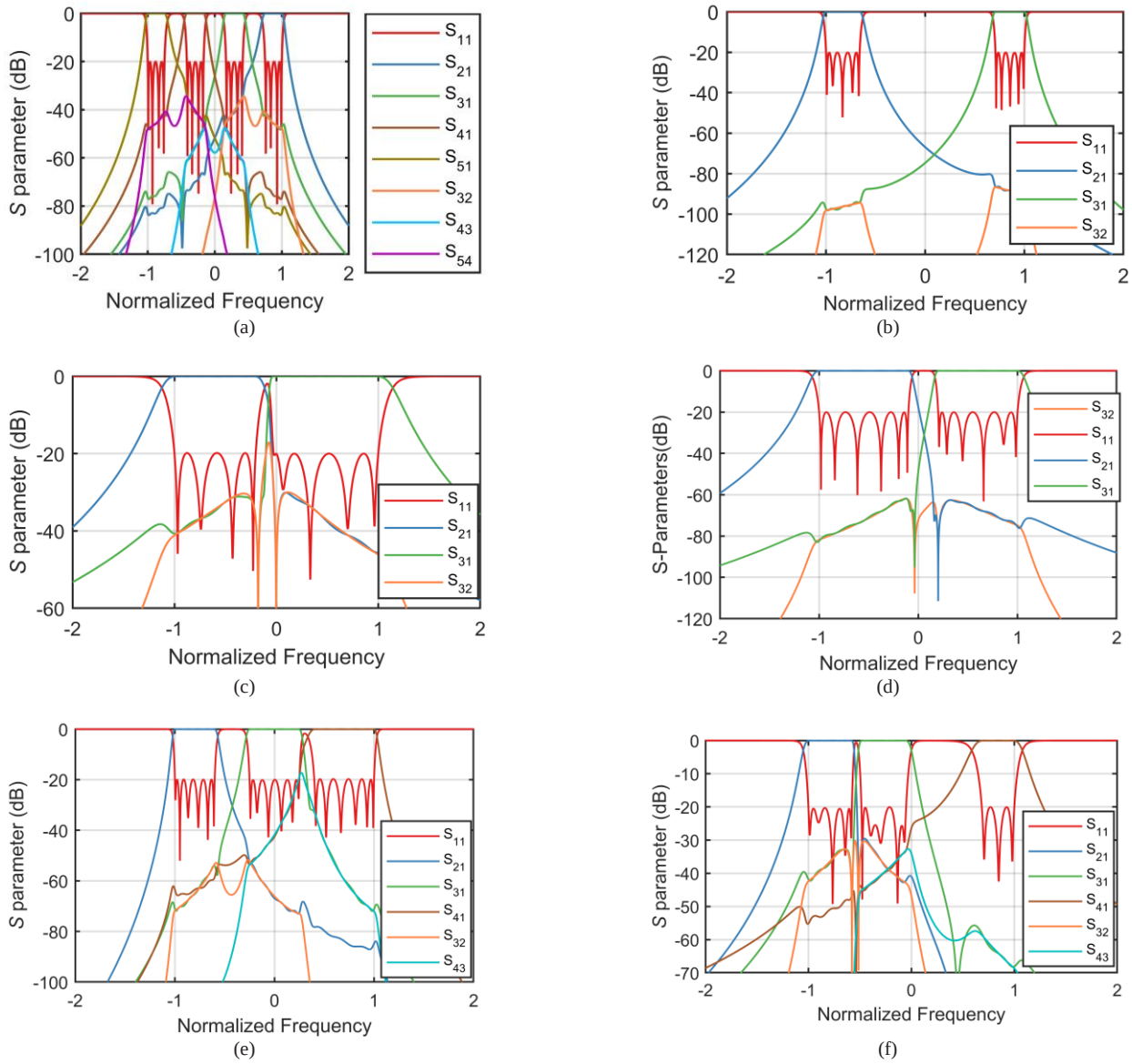

Fig. 11. Responses of the optimal solutions by GACMS for the six test cases. (a) Example 1; (b) Example 2; (c) Example 3; (d) Example 4; (e) Example 5; (f) Example 6.

TABLE VII
The statistics of the GACMS results over 10 runs

Problems	Optimal objective function values			
	Min	*Max*	*Mean*	*STD*
1	8.67E−3	8.76E−3	8.70E−3	3.24E−5
2	0.00E0	0.00E0	0.00E0	0.00E0
3	8.69E−3	2.19E−2	1.18E−2	3.99E−3
4	0.00E0	0.00E0	0.00E0	0.00E0
5	1.38E−2	6.09E−2	3.08E−2	1.38E−2
6	0.00E0	0.00E0	0.00E0	0.00E0

specifications (i.e., cost function = 0), and the other examples also obtain excellent results. Moreover, the very small standard deviation over the 10 runs shows the robustness of GACMS. In the response of Fig. 11(d) for the topology of Fig. 10(d), it may be observed that only two transmission zeros are clearly identifiable. This happens because the two transmission zeros introduced by the coupling clusters 1-4 almost merge into the two zeros from the channel triplets. The four transmission zeros are clearly visible from a sub-optimal solution (with slightly lower rejection at the band-edge), which is not shown here.

B. Comparisons with State-of-the-art Methods

As mentioned earlier, although CM synthesis is well established for filters, it is far from mature for all-resonator diplexers and multiplexers. The most popular and probably the only general optimization-based method is SQP with the starting point based on experience [14]. SADEC is an optimizer for diplexer synthesis instead of a standalone methodology [15]. The goal of SADEC is to reduce the high dependency on the starting point, but it still needs to be implemented in a CM synthesis framework. Therefore, the reference method that we choose is SQP.

The quality of the starting point determines the success of SQP-based CM synthesis. To ensure the starting point quality, we use the following settings: For the coupling coefficients in the branches, the FK values from Step 2 of GACMS are used. For the coupling coefficients in the stem, because there is no FK value, 0.5 is used as in other filter synthesis methods [23]. To avoid destroying the optimal pattern as discussed in section III, the search ranges are the same as GACMS for the coupling coefficients in the branches. It can be seen that this comparison favors SQP by taking advantage of some ideas borrowed from GACMS. SQP is implemented using the function "fmincon" in MATLAB [26]. Since SQP is a deterministic method, only one run is needed. Table VIII compares the optimal objective function values of the enhanced SQP and the average objective function values of GACMS. Table IX shows the success rate of the two methods. The success of CM synthesis is judged based on the following rules [15]: (1) The reflection zeros are located within the specified channel passbands. (2) The S-parameter specifications are satisfied or almost satisfied (i.e., $\max|S_{11}| < -18$dB). It can be seen that the final objective function values of GACMS are better than that of enhanced SQP for all the cases. The enhanced SQP fails for the more complicated cases 4-6 in contrast with the 100% success rate for GACMS.

For the cases 4-6, it is observed that the enhanced SQP is trapped in an unacceptable local optimum which is not near to the appropriate coupling coefficients. This shows that even with a carefully selected starting point, the optimization ability of SQP is insufficient for the targeted complex cases. The difference in terms of complexity between filter and diplexer / multiplexer CM synthesis can also be observed. When using 0.5 as the starting point for all the variables, two-port filter CM synthesis using SQP often succeeds [24], but it is not the case for diplexers and multiplexers with complex structures.

TABLE VIII
Comparison of optimal objective function values from enhanced SQP and GACMS (average) for the test cases

Problems	Methods	Objective function values
1	SQP	0.0128
	GACMS	0.00870
2	SQP	0.152
	GACMS	0.00
3	SQP	0.391
	GACMS	0.0118
4	SQP	0.996
	GACMS	0.00
5	SQP	0.501
	GACMS	0.0308
6	SQP	1.87
	GACMS	0.00

TABLE IX
Success rate of enhanced SQP and GACMS for the test cases

Problems	Methods	
	SQP	GACMS
1	100%	100%
2	100%	100%
3	100%	100%
4	0%	100%
5	0%	100%
6	0%	100%

C. Verification of the Advantages of MSADEC

This subsection focuses on verifying the advantages of the new MSADEC algorithm over the original SADEC in [15]. Using the same synthesis framework described in Section III (B), the Optimizer I (MSADEC) used in Step 4 is replaced by the original SADEC in [15]. All the parameter settings are the same. Ten runs are carried out for each test case and the comparison results are shown in Table X and Table XI.

It can be seen that when using the original SADEC as Optimizer I, although the result is better than SQP, the solution quality is clearly worse than that of MSADEC. For one thing, the optimal objective function values obtained by MSADEC are much smaller than SADEC for all the test cases. For the very complex test cases 5 and 6, the success rate of SADEC drops. For test case 6, only 3 out of 10 runs succeed when using SADEC, in contrast with the 100% success rate of MSADEC.

Another observation is that when using MSADEC, the convergence often occurs within 20,000 evaluations, while SADEC needs more than 200,000 evaluations. This can be explained by the landscape in Fig. 2. SADEC is a global optimization algorithm. When the narrow valley that contains the global optimum is identified, the DE mutation operator may destroy the already obtained optimal pattern and generate candidate solutions in the flat region in Fig. 2. This is because the valley is too narrow compared to the step size of the DE

TABLE X
The optimal objective function values of the test cases using MSADEC and SADEC based on the GACMS framework

Problems	Methods	Optimal objective function values			
		Min	*Max*	*Mean*	*STD*
1	SADEC	0.0106	0.0360	0.0215	0.00791
	MSADEC	0.00867	0.00876	0.00870	0.0000324
2	SADEC	0.0520	0.113	0.0652	0.0175
	MSADEC	0.00	0.00	0.00	0.00
3	SADEC	0.0589	0.0745	0.0691	0.00439
	MSADEC	0.00869	0.0219	0.0118	0.00399
4	SADEC	0.0038	0.0237	0.0128	0.00671
	MSADEC	0.00	0.00	0.00	0.00
5	SADEC	0.117	0.268	0.179	0.0486
	MSADEC	0.0138	0.0609	0.0308	0.0138
6	SADEC	0.0241	0.595	0.275	0.166
	MSADEC	0.00	0.00	0.00	0.00

TABLE XI
The success rate of the test cases using MSADEC and SADEC in GACMS

Problems	Methods	
	GACMS+SADEC	GACMS+MSADEC
1	100%	100%
2	100%	100%
3	100%	100%
4	100%	100%
5	90%	100%
6	30%	100%

mutation at some search phases. Only when the candidate solutions in the population are near to each other (i.e., near the convergence), the step size becomes appropriate. In other words, SADEC is in the process of "making and breaking". In contrast, MSADEC utilizes a local search (also with restricted search ranges) to improve the objective function while protecting the existing optimal pattern.

VI. Conclusions

In this paper, a CM synthesis method for all-resonator diplexers and multiplexers, called GACMS, has been proposed. GACMS is believed to be the first general method to address complex CM synthesis of all-resonator diplexers and multiplexers. Case studies and comparisons show its high optimization ability and robustness for the targeted complex CM synthesis problem. The excellent performance of the method can be attributed to the new framework, which applies filter design knowledge to reduce the search ranges simplifying the optimization problem, and the new MSADEC optimizer which addresses the challenges of the particular landscape. The six practical examples are used not only to demonstrate the capability of GACMS, but also to provide for future tests and comparisons for the community.

A limitation of GACMS is the number of channels to be handled. The larger the number of channels, the more resonators need to be included in the frequency distribution network. The coupling coefficients around those junction resonators do not usually have the FK values, and have to be searched over the full range, e.g., [0,1]. Hence, the search space can be substantially enlarged. Our experience found that GACMS has successfully synthesized CM for multiplexers with up to about 7 channels. Our future work will focus on overcoming the current limitation and developing software tools based on GACMS.

Appendix

The external couplings, FK values and optimization results for Example 1-6 are listed in the following.

A. Example 1

External couplings	m(P1,1)=0.7327, (P2,7)=m(P3,10)=m(P4,13)=m(P5,16)=0.3663.
FK values	m(5,6)=m(8,9)=0.0876, m(6,7)=m(9,10)=0.1140, m(5,5)=m(6,6)=m(7,7)=0.8750; m(8,8)=m(9,9)=m(10,10)=0.2920
Final solution	m(1,2)=0.7249, m(2,3)=m(2,4)=0.4006, m(3,5)=m(4,14)=0.1736, m(5,6)=m(14,15)=0.0926, m(6,7)=m(15,16)=0.1147, m(3,8)=m(4,11)=0.1318, m(8,9)=m(11,12)=0.0887, m(9,10)=m(12,13)=0.1142, m(1,1)=m(2,2)=0, m(3,3)=0.4479, m(4,4)=−m(3,3), m(5,5)=0.8203, m(6,6)=0.8674, m(7,7)=0.8715, m(14,14)=−m(5,5), m(15,15)=−m(6,6), m(16,16)=−m(7,7), m(8,8)=0.3033, m(9,9)=0.2933, m(10,10)=0.2927, m(11,11)=−m(8,8), m(12,12)=−m(9,9), m(13,13)=−m(10,10).

B. Example 2

External couplings	m(P1,1)=0.5696, m(P2,6)=0.4177, m(P3,10)=0.3874.
FK values	m(3,4)=0.1078, m(4,5)=0.1078, m(5,6)=0.1468, m(7,8)=0.0927, m(4,5)=0.0927, m(5,6)=0.1262, m(3,3)=m(4,4)=m(5,5)=m(6,6)=−0.8306; m(7,7)=m(8,8)=m(9,9)=m(10,10)= 0.8543.
Final solution	m(1,2)= 0.8688, m(2,3)= 0.2133, m(3,4)= 0.1100, m(4,5)=0.1076, m(5.6)= 0.1474, m(2,7)=0.1653, m(7,8)=0.0921, m(8,9)=0.0929, m(9,10)=0.1255 m(1,1)=−0.0729, m(2,2)=0.0797, m(3,3)=−0.8060, m(4,4)=−0.8280, m(5,5)=−0.8288, m(6,6)=−0.8241, m(7,7)=0.8384, m(8,8)=0.8532, m(9,9)=0.8540, m(10,10)=0.8512.

C. Example 3

External couplings	m(P1,1)=0.9362, m(P2,5)=0.6112, m(P3,10)=0.7092.
FK values	m(2,3)=0.2976, m(3,4)=0.2189, m(4,5)=0.3618, m(2,4)=−0.2058 m(6,7)=0.2664, m(7,8)=0.2664, m(8,9)=0.4421, m(6,8)=0.1885, m(2,2)=−0.6283, m(3,3)=−0.3441, m(4,4)=−0.6469, m(5,5)=−0.6283, m(6,6)=0.5107, m(7,7)=0.1725, m(8,8)=0.5107, m(9,9)=0.5040.
Final solution	m(1,2)= 0.5779, m(2,3)= 0.2461, m(3,4)= 0.2107, m(4,5)= 0.3592, m(1,6)= 0.5985, m(6,7)= 0.2702, m(7,8)= 0.2673, m(8,9)= 0.4419, m(2,4)= −0.1726, m(6,8)= 0.1961 m(1,1)= 0.0113, m(2,2)= −0.5377, m(3,3)=−0.3027, m(4,4)=−0.6177, m(5,5)=− 0.6114, m(6,6)= 0.5014, m(7,7)= 0.1778, m(8,8)= 0.5217, m(9,9)= 0.5185.

D. Example 4

External couplings	m(P1,1)=0.9232, m(P2,5)=0.6720, m(P3,10)=0.6330.
FK values	m(2,5)=0.2550, m(5,6)= 0.2344, m(6,7)= 0.2524, m(7,8)= 0.3825 m(2,4)=0.2614, m(5,7)=−0.1020, m(1,4)= 0.8719, m(3,9)=0.2251, m(9,10)= 0.2101, m(10,11)= 0.2251, m(11,12)= 0.3316, m(3,4) = 0.2343, m(9,11) = 0.0814, m(2,2)= −0.5769, m(3,3)= 0.6167, m(5,5)=−0.5709, m(6,6)=−0.3715, m(7,7)= −0.5604, m(8,8)= −0.5667, m(9,9)= 0.6136, m(10,10)= 0.4548, m(11,11)= 0.6052, m(12,12)= 0.6046.
Final solution	m(1,2)=−0.3438, m(2,5)=0.2700, m(5,6)= 0.2343, m(6,7)= 0.2490, m(7,8)= 0.3793, m(2,4)= 0.1725, m(5,7)= −0.1153, m(1,4)= 0.6542, m(3,9)= 0.3226,

	m(9,10)= 0.2083, m(10,11)= 0.2225, m(11,12)= 0.3377, m(3,4) = 0.1496, m(9,11) = 0.1023, m(1,1)= −0.0066, m(2,2)=−0.5866, m(3,3)=0.6370,m(4,4)=0.0505, (5,5)=−0.5719, m(6,6)=−0.3476, m(7,7)=−0.5600, m(8,8)=−0.5578, m(9,9)=0.6212, m(10,10)= 0.4205, m(11,11)= 0.6072, m(12,12)= 0.6025.

E. Example 5

External couplings	m(P1,1)=0.8686, m(P2,14)=0.4486, m(P3,8)=0.5015, m(P4,18)=0.5494.
FK values	m(4,5)= 0.1528, m(5,6)= 0.1459, m(6,7)= 0.1528, m(7,8)= 0.2109 m(11,12)= 0.1272, m(12,13)= 0.1272, m(13,14)= 0.1732 m(15,16)=0.1908, m(16,17)=0.1908, m(17,18) = 0.2599 m(4,4)=m(5,5)=m(6,6)=m(7,7)=m(8,8) =0.0 m(11,11)=m(12,12)=m(13,13)=m(14,14) = −0.8 m(15,15)=m(16,16)=m(17,17)=m(18,18)=0.7
Final solution	m(1,2)=0.7597, m(2,3)= 0.5753, m(3,4) = 0.2801 m(4,5)= 0.1557, m(5,6)= 0.1451, m(6,7)= 0.1522, m(7,8)= 0.2108, m(3,9) = 0.4151, m(9,10)= 0.6737, m(10.11)= 0.1804, m(11,12)= 0.1195, m(12,13)= 0.1230, m(13,14)= 0.1692, m(10,15) = 0.3003, m(15,16)= 0.1854, m(16,17)= 0.1867, m(17,18) = 0.2546 m(1,1)= 0.0622, m(2,2)= −0.0369, m(3,3)= 0.0361, m(4,4)=−0.0051, m(5,5)= −0.0052, m(6,6)= −0.0034, m(7,7)= −0.0028, m(8,8)= −0.0038, m(9,9)= 0.0345, m(10,10)=−0.0961 m(11,11)= −0.7730, m(12,12)= −0.7948, m(13,13)= −0.7947, m(14,14) = −0.7959, m(15,15)= 0.6216, m(16,16)= 0.6806, m(17,17)= 0.6894, m(18,18)= 0.6896

F. Example 6

External couplings	m(P1,10=0.5, m(P2,5)=0.4541, m(P3,9)=0.5125, m(P4,13)=0.4352.
FK values	m(2,3)=0.1143, m(3,4)=0.1143, m(4,5)=0.1816, m(2,4)=−0.0697 m(1,1)=−0.7957, m(2,2)=−0.7983, m(3,3)=−0.6726,m(4,4)=−0.7983, m(5,5)=−0.7957, m(6,7)= 0.1394, m(7,8) = 0.1394, m(8,9)=0.2309, m(6,8)=0.0981, m(6,6)=−0.2043, m(7,7)=−0.3804, m(8,8)=−0.2043, m(9,9)=−0.2078, m(11,12)=0.1684, m(12,13) =0.1684, m(11,11)=m(12,12)=m(13,13)= 0.8368
Final solution	m(1,2)=0.2000, m(2,3)=0.1069, m(3,4)=0.1065, m(4,5)=0.1786, m(2,4)=−0.0831 m(1,1)=−0.5253, m(2,2)=−0.7720, m(3,3)=−0.6502, m(4,4)=−0.7970, m(5,5)=−0.7889, m(10,1) = 0.4853 , m(1,6) = 0.2045 m(6,7)= 0.1163, m(7,8) = 0.1160, m(8,9)=0.2013, m(6,8)=0.0780, m(6,6)=−0.2964, m(7,7)=−0.4042, m(8,8)=−0.2606, m(9,9)=−0.2706, m(10,11)=0.6019, m(11,12)=0.1794, m(12,13) =0.1661, m(10,10)= −0.1501, m(11,11)= 0.5523, m(12,12)= 0.8172, m(13,13)= 0.8330

REFERENCES

[1] R. J. Cameron, C. M. Kudsia, and R. R. Mansour, *Microwave filters for communication systems: fundamentals, design, and applications*. Wiley-Interscience, 2007.

[2] J. W. Bandler, Q. S. Cheng, N. K. Nikolova, and M. A. Ismail, "Implicit space mapping optimization exploiting preassigned parameters," *IEEE Trans. Microw. Theory Tech.*, vol. 52, no. 1, pp. 378–385, Jan. 2004.

[3] B. Liu, H. Yang, and M. J. Lancaster, "Global optimization of microwave filters based on a surrogate model-assisted evolutionary algorithm," *IEEE Trans. Microw. Theory Techn.*, vol. 65, no. 6, pp. 1976–1985, Jun. 2017.

[4] J. -S. G. Hong and M. J. Lancaster, *Microstrip Filters for RF/Microwave Application*, vol. 167. Hoboken, NJ, USA: Wiley, 2004.

[5] G. Macchiarella and S. Tamiazzo, "Novel approach to the synthesis of microwave diplexers," *IEEE Trans. Microw. Theory Techn.*, vol. 54, no. 12, pp. 4281–4290, Dec. 2006.

[6] G. Macchiarella and S. Tamiazzo, "Synthesis of star-junction multiplexers," *IEEE Trans. Microw. Theory Techn.*, vol. 58, no. 12, pp. 3732–3741, Dec. 2010.

[7] P. Zhao and K.-L. Wu, "An iterative and analytical approach to optimal synthesis of a multiplexer with a star-junction," *IEEE Trans. Microw. Theory Techn.*, vol. 62, no. 12, pp. 3362–3369, Dec. 2014.

[8] X. Shang, Y. Wang, W. Xia, and M. J. Lancaster, "Novel Multiplexer Topologies Based on All-Resonator Structures," *IEEE Trans. Microw. Theory Tech.*, vol. 61, no. 11, pp. 3838-3845, 2013.

[9] T. Skaik, M. Lancaster, M. Ke, and Y. Wang, "A micromachined WR-3 band waveguide diplexer based on coupled resonator structures," in *2011 41st European Microwave Conference*, 2011, pp. 770-773.

[10] R. Wang, J. Xu, M.-Y. Wang, and Y.-L. Dong, "Synthesis of microwave resonator diplexers using linear frequency transformation and optimization," *Progress In Electromagnetics Research*, vol. 124, pp. 441-456, 2012.

[11] I. Llamas-Garro, F. Mira, P. Zheng, Z. Liu, L. Wu, and Y. Wang, "All-resonator based LTCC diplexer using substrate-integrated-waveguides," *Electronics Letters*, vol. 53, no. 21, pp. 1410-1412, 2017.

[12] S. Tamiazzo and G. Macchiarella, "Synthesis of diplexers with the common port matched at all frequencies," *IEEE Trans. Microw. Theory Techn.*, vol. 62, no. 1, pp. 46–54, Jan. 2014.

[13] G. Macchiarella and S.Tamiazzo, "Generation of canonical forms for multiport filtering networks," in *IEEE MTT-S Int. Microw. Symp. Dig.*, Jun. 2014, pp. 1-3.

[14] T. F. Skaik, M. J. Lancaster, and F. Huang, "Synthesis of multiple output coupled resonator circuits using coupling matrix optimisation," *IET Microwaves Antennas Propag.*, vol. 5, no. 9, pp. 1081-1088, 2011.

[15] B. Liu, H. Yang, and M. J. Lancaster, "Synthesis of coupling matrix for diplexers based on a self-Adaptive differential evolution algorithm," *IEEE Transactions on Microwave Theory and Techniques*, vol. 66, no. 2, pp. 813-821, 2018.

[16] W. Xia, "Diplexers and multiplexers design by using coupling matrix optimization," Ph.D. dissertation. Dept. Elect. Eng, Birmingham Univ., Birmingham, U.K., 2015.

[17] Y. Wu, Y. Wang and E. A. Ogbodo, "Microstrip wideband diplexer with narrow guard band based on all-resonator structures," in 2016 46th European Microwave Conference (EuMC), London, United Kingdom, 2016, pp. 1163-1166.

[18] K. Price, R. M. Storn, and J. A. Lampinen, *Differential evolution: a practical approach to global optimization*. Springer Science & Business Media, 2006.

[19] P. T. Boggs and J. W. Tolle, "Sequential quadratic programming," Acta numerica, vol. 4, pp. 1-51, 1995.

[20] S. Wright and J. Nocedal, *Numerical optimization*, Springer Science, vol. 35, no. 67-68, p. 7, 1999.

[21] B. Liu, H. Yang, and M. J. Lancaster, "Global Optimization of Microwave Filters Based on a Surrogate Model-Assisted Evolutionary Algorithm," *IEEE Trans. Microw. Theory Tech.*, vol. 65, no. 6, pp. 1976-1985, 2017.

[22] R. J. Cameron, "Advanced coupling matrix synthesis techniques for microwave filters," *IEEE Trans. Microw. Theory Tech.*, vol. 51, pp. 1–10, Jan. 2003.

[23] S. Amari, "Synthesis of cross-coupled resonator filters using an analytical gradient-based optimization technique," *IEEE Trans. Microw. Theory Tech.*, vol. 48, no. 9, pp. 1559-1564, 2000.

[24] P. Moscato, "On evolution, search, optimization, genetic algorithms and martial arts: Toward memetic algorithms," in "Caltech Concurrent Computation Program," California Inst. Technol., Pasadena, CA, Tech. Rep. 826, 1989.

[25] Y. Wu, R. Wu and Y. Wang, "A Compact Coupling Structure for Diplexers and Filtering Power Dividers," *Progress In Electromagnetics Research*, vol. 69, pp. 161-170, 2018.

[26] MATLAB Optimization ToolboxTM. User's guide, MATLAB, Natick, Massachusetts, www.mathworks.com (accessed 2 May 2018).

Yang Yu was born in Tianjin, P.R.China, in 1991. He received the B.Eng. degree in communication engineering and the M.Eng. degree in information and communication engineering at Tianjin Polytechnic University, Tianjin, P.R.China, in 2013 and 2016, respectively. He is currently pursuing the Ph.D. degree at University of Birmingham, Birmingham, U.K.. He is now a joint Ph.D. student with the University of Birmingham, Birmingham, U.K., and Southern University of Science and Technology, Shenzhen, P.R.China. His recent research focuses on synthesis and design of RF/microwave components and computational intelligence techniques for engineering.

Bo Liu (M'15-SM'17) received the B.S. degree from Tsinghua University, P. R. China, in 2008. He received his Ph.D. degree at University of Leuven (KU Leuven), Belgium, in 2012. From 2012 to 2013, he was a Humboldt research fellow and was working with Technical University of Dortmund, Germany. In 2013, he was appointed Lecturer at Wrexham Glyndwr University, UK, where he was promoted to Reader in 2016. Since 2020, he is a Senior Lecturer at University of Glasgow, UK. He is also an honorary fellow at University of Birmingham, UK. His research interests lie in AI-driven design methodologies of analog/RF integrated circuits, microwave devices, MEMS, evolutionary computation and machine learning. He has authored or co-authored 1 book and more than 60 papers in renowned international journals, edited books and conference proceedings.

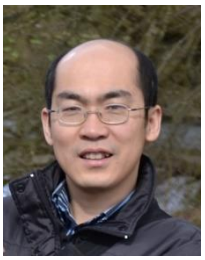

Yi Wang (M'09–SM'12) was born in Shandong, China. He received the B.Sc. degree in physics and M.Sc. degree in condensed matter physics from the University of Science and Technology, Beijing, China, in 1998 and 2001, respectively, and the Ph.D. degree in electronic and electrical engineering from the University of Birmingham, Edgbaston, Birmingham, U.K., in 2005. In 2011, he became a Senior Lecturer and then Reader at the University of Greenwich. In 2018, Yi joined Birmingham as a Senior Lecturer. His current research interests include millimeter-wave and terahertz devices for metrology, communications and sensors, micromachining, microwave circuits based on multiport filtering networks, and filter-antenna integration.

Michael J. Lancaster (SM'2004) was born in England in 1958. He was educated at Bath University, UK, where he graduated with a degree in Physics in 1980. His career continued at Bath, where he was awarded a PhD in 1984 for research into non-linear underwater acoustics.

After leaving Bath University he joined the surface acoustic wave (SAW) group at the Department of Engineering Science at Oxford University as a Research Fellow. The research was in the design of new, novel SAW devices, including RF filters and filter banks. In 1987 he became a Lecturer at The University of Birmingham in the Department of Electronic and Electrical Engineering, lecturing in electromagnetic theory and microwave engineering. Shortly after he joined the department he began the study of the science and applications of high temperature superconductors, working mainly at microwave frequencies. He was promoted to head of the Department of Electronic, Electrical and Systems Engineering in 2003. His present personal research interests include microwave filters and antennas, as well as the high frequency properties and applications of a number of novel and diverse materials. This includes micromachining as applied to terahertz communications devices and systems.

Professor Lancaster is Fellow of the IET and UK Institute of Physics. He is a Chartered Engineer and Chartered Physicist. He has served on MTT IMS technical committees. Professor Lancaster has published two books and over 200 papers in refereed journals.

Qingsha S. Cheng (S'00–M'05–SM'09) received the B.Eng. and M. Eng. from Chongqing University, China, in 1995 and 1998, respectively. He received his Ph.D. at McMaster University, Canada, in 2004. In 1998, he was with the Department of Computer Science and Technology, Peking University, China. In 2004, he became a postdoctoral fellow and then a research engineer in 2007, both with the Department of Electrical and Computer Engineering, McMaster University. In 2014, he joined Southern University of Science and Technology (SUSTech), Shenzhen, China as an assistant professor in the Department of Electrical and Electronic Engineering. His research interests include surrogate modeling, computer-aided design and tuning, efficient design and modeling of microwave circuits, and novel materials and fabrication technologies. He has authored or co-authored more than 100 publications in technical book chapters, refereed international technical journals, refereed international conference proceedings and international workshops. His works have been cited more than 2500 times according to Google scholar.